CEAS Space Journal
https://doi.org/10.1007/s12567-024-00564-w

ORIGINAL PAPER

Selection of propulsion characteristics for systematic assessment of future European RLV-options

Martin Sippel[1] · **Jascha Wilken**[1]

Received: 31 December 2023 / Revised: 31 July 2024 / Accepted: 19 August 2024
© The Author(s) 2024

Abstract
The propulsion system as the key-element of any space transportation concept is systematically investigated supporting a study on potential future European RLV. Different liquid propellant combinations are compared and evaluated. Subsequently, main stage rocket engines are defined for the two cycle options: open gas-generator and closed staged-combustion. Four different propellant combinations are considered all based on liquid oxygen (LOX) as oxidizer and with the fuel options liquid hydrogen (LH2), liquid methane (LCH4), liquid propane (LC3H8) and kerosene (RP1). These combinations result in eight different generic engines with sub-variants using different nozzle expansion ratios in first and upper stage application. Engine characteristics are similar, as far as conceivable, to be well-suited for the system level comparison of pre-defined RLV-launchers. However, characteristics are not necessarily identical as different engine architectures and propellants might make individual choices necessary. Engine performance characteristics are compared with similar existing engines when available. It is shown that closed-cycle staged combustion engines bring significant performance gains, particularly in sea-level operations. On the other hand, hydrocarbon- and open-cycle gas-generator engines offer a better thrust-to-weight-ratio than hydrogen and staged combustion cycle.

Keywords Rocket propulsion · Rocket propellants · Staged combustion cycle · Gas generator cycle

Abbreviations

A	(Cross section) area m^2
I_{sp}	(Mass) specific Impulse s (N s / kg)
M	Mach-number
p	Pressure MPa (bar)
T	Thrust N
m	Mass kg
W	Weight N
ε	Expansion ratio
FFSC	Full-flow staged combustion
FRSC	Fuel-rich staged combustion
FTP	Fuel turbo pump
LC3H8	Liquid propane
LCH4	Liquid methane
LH2	Liquid hydrogen
LOX	Liquid oxygen
MCC	Main combustion chamber
MR	Mixture ratio
N.B.	Nota bene
OTP	Oxidizer turbo pump
ORSC	Oxidizer-Rich staged combustion
RP1	Rocket propellant (Kerosene)
SLME	SpaceLiner Main Engine
SSME	Space shuttle main engine
TET	Turbine entry temperature
VTHL	Vertical take-off horizontal landing
VTVL	Vertical take-off vertical landing
c, C	Chamber
fr	Frozen
s/l	Sea level
t	Throat
vac	Vacuum

1 Introduction

Reusability of launch systems is the key innovation element in early twenty-first century space transportation. The US-American-company SpaceX has demonstrated with Falcon 9 Block 5 that routine operation with multiple reuses of first stages is feasible and probably also cost effective. This major

✉ Martin Sippel
Martin.Sippel@dlr.de

[1] Space Launcher Systems Analysis (SART), DLR, Bremen, Germany

Published online: 18 September 2024

achievement by SpaceX shows one technical option, however, not necessarily the best technical option for Europe with its different mission scenario.

The Space Launcher System Analysis division SART of the German Aerospace Center (DLR) has performed a systematic investigation of promising options for a reusable first stage of a future European partially reusable launch vehicle. The final goal has been the determination of the impact of the different return methods on a technical, operational and economical level and the assessment of their relevance for a future European launch system. Within the first phase (called ENTRAIN 1, see also [1–4]) a wide variety of reusable first stages were investigated by DLR. This includes vertical take-off vertical landing (VTVL) with propulsive deceleration [2] and vertical take-off horizontal landing (VTHL) with winged stages and aerodynamic deceleration in the atmosphere [3].

The systematic assessment of future RLV-stages and technical options requires the definition of generic engines with similar baseline assumptions in order to reach maximum comparability. The underlying assumptions of all propulsion aspects and justification of certain choices are in focus of this paper. This includes an overview on the propellants and important engine performance characteristics which are compared to existing engines, whenever possible. Such cross validation is essential to generate realistic engine reference data to be used in a viable and meaningful preliminary launcher sizing.

The available literature on comparable engine data for different fuel choices and engine cycles is limited, even more so when considered from a European perspective. While comparative data for the combustion chamber performance alone is available for various propellant combinations in established literature [5], it doesn't contain generic data based on the analysis of entire engine cycles. In previous system optimization studies [6] the performance of closed cycles was derived from the combustion chamber performance without a detailed analysis of the entire cycle, while for the gas generator cycle the massflow through the gas generator was estimated via a regression over the combustion chamber pressure. The latter approach has the disadvantages of neither considering the individual propellant characteristics, gas generator conditions, nor the turbomachinery efficiencies and pressure ratios. A former DLR study already looked into the launcher system performance of entire engine cycles [7, 8], however, at the time was focused only on staged combustion methane and kerosene rocket engines. Another study with an industrial perspective on hydrocarbon propellants has been published as a conference paper [9].

In contrast to existing literature this manuscript aims to provide a database for staged combustion and gas generator rocket engines for four different fuel options (hydrogen, methane, propane and kerosene), all evaluated under realistic and comparable assumptions for the engine cycle and thrust chamber performance.

2 Propellants

The main driver for chemical rocket engines to achieve high performance is by selection of the propellant combination. As long as thrust-levels are scaled with the engine massflow without running into design challenges, the (mass) specific impulse I_{sp} is representing chemical engine performance. Additional criteria are to be considered which are important but, nevertheless, are secondary to performance dominating spaceflight. These other high-level criteria for propellants are

- non- or low-toxicity of the propellants or reaction products,
- low or at least affordable production costs of the propellants,
- simple handling in ground operations and hence low operating costs, and not to forget
- energy efficiency in production, low environmental and climate impact (e.g. in CO_2-equivalent)

It is well known that a compromise is to be found as no propellant combination has been identified fulfilling always the optimum conditions. In case of reusable stages only liquid-state propellant combinations are of interest. The easily available and cheap oxidizer is liquid oxygen (LOX) and corresponding fuels of interest are:

- Liquid hydrogen (LH2) and the hydrocarbons
- Liquid methane (LCH4)
- Liquid propane (LC3H8)
- Kerosene or rocket propellant (RP1)

These four fuels in combination with oxygen are most promising for modern launcher application and are selected for this study without performing extensive trade-offs with more exotic alternative fuels or oxidizers. The reason these propellant combinations are widely used, or at least being under extensive study is the fact that the high-level criteria listed are well met.

2.1 Key characteristics at typical operating points

Note, all propellants with the only exception RP1 would be in gaseous state under the ambient conditions at all possible launch sites. For the practical use in launch vehicles, these propellants need to be liquified by significant cooling below ambient temperature which is represented

Table 1 Key propellant characteristics [10, 12]

	LOX	LH2	LCH4	LC3H8	RP1
Molar mass [g/Mol]	31.9988	2.01588	16.04	44.1	13.97
Typical tank filling conditions (1 bar pressure at sea-level)					
Temperature [K]	90.1	20.324	111.66	231.08	298.1
Density [kg/m^3]	1141.8	70.899	422.6	582	807
Thermodynamic characteristics					
Normal melting point [K]	54.361	13.957	90.68	85.47	223
Normal boiling point [K]	90.1878	20.369	111.63	231.08	400–500
Critical temperature [K]	154.581	33.145	190.5	369.8	956
Critical pressure [MPa]	5.043	1.2964	4.596	4.25	2.18
Critical density [kg/m^3]	436.1	31.262	162.8	224.9	232.3
Combustion heat [kJ/kg]	–	120,000	55,526	50,327	43,340

Table 2 Stoichiometric mixture ratio (MR) of propellants with LOX

LH2	LCH4	LC3H8	RP1
7.936	3.989	3.628	3.403

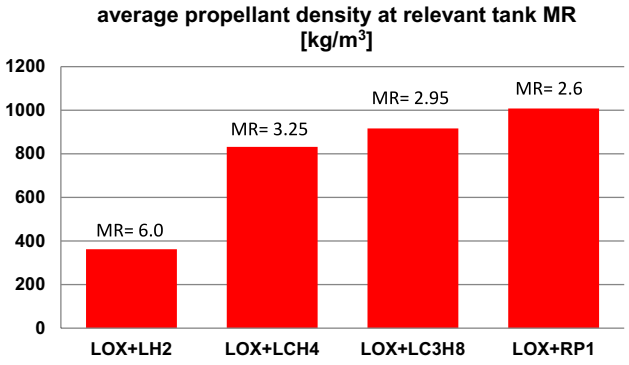

Fig. 2 Average density inside tanks of propellant combinations with LOX

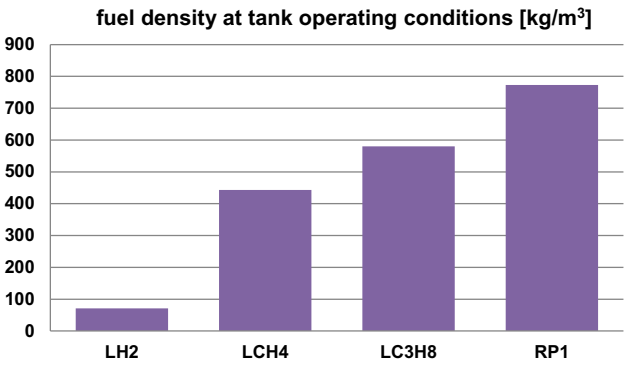

Fig. 1 Density at normal boiling point for cryogenic fuels and at ambient temperature for RP1

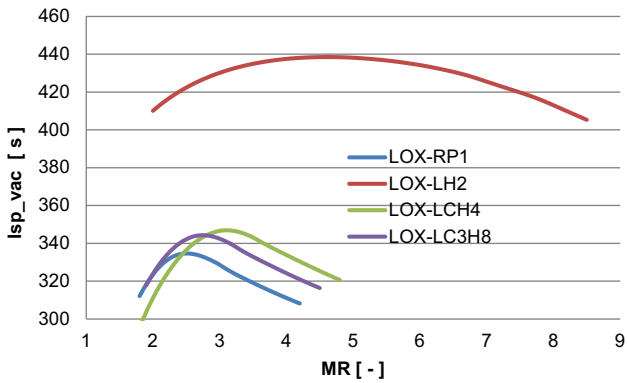

Fig. 3 I_{sp} in vacuum as function of mixture ratio (MR) and different propellant combinations calculated for main combustion chamber

by the capital letter L in the names. Characteristic data are listed in Table 1.

The three hydrocarbon fuels methane, kerosene (RP1), and propane are relatively close in their characteristics. Methane represents the lowest density of the hydrocarbon propellants while Kerosene embodies the highest density. Kerosene (RP1) is more than 10 times denser than liquid hydrogen and even methane is about 6 times more dense than the lightest element at normal boiling point (Fig. 1).

The most commonly used oxidizer in launch vehicles is liquid oxygen (LOX) with a density at normal boiling point (90.15 K, 1 bar) at 1142 kg/m^3. Relevant for stage sizing is not the density of the fuels alone (as shown in Fig. 1) but the average bulk density of the two propellant constituents, oxidizer and fuel at the resp. relevant mixture ratio (MR). MR of practical engines remain below the stoichiometric values listed in Table 2 and are defined with the engine investigations in Sects. 3.2–3.6. The lighter the fuel, the higher the mixture ratio and hence amount of relatively dense and heavy oxygen in the propellant combination. As a result, the average propellant density shows the same ranking order but much less pronounced with a factor of 2.5 between densest LOX-RP1 compared to LOX-LH2 (Fig. 2).

Figure 3 shows the dependency of vacuum specific impulse on the propellant mixture ratio calculated for chamber pressure p_c of 16 MPa and nozzle expansion ratio ε of 33. These are typical data, later being used in the work as a reference for the preliminary sizing of engines. Note the relatively close position of all hydrocarbon fuels compared to hydrogen and that the optimum I_{sp}-performance is found for all propellants below the stoichiometric MR as listed in

Table 2 because lighter molecules in the exhaust composition shift somehow the optimum position.

2.2 Relevant internal engine fuel characteristics

The following short summary of fuel characteristics is relevant for the correct and safe functioning of rocket engines. These play a minor role in the performance estimation and engine preliminary sizing but important to be kept in mind anticipating more detailed engine definition.

2.2.1 Thermal stability and coking

The decomposition of hydrocarbons takes place when a certain fluid temperature is exceeded in the case of heat transfer. Due to a defined property of the fuel for the combustion process and as coolant in the regenerative cooling system, this has to be prevented. Certain bulk- and wall temperature limitations have to be considered.

Thermal cracking of hydrocarbons is dependent on wall temperatures, flow rates and pressure. Molecules with higher atomic mass can be decomposed at lower heat input. It has been observed that higher pressures decrease the tendency of thermal decomposition of propellants and the temperature value for starting thermal decomposition is shifted towards higher values as the pressure is increased [10].

Coking is the deposition of carbon compounds to the cooling channel wall. These layers are increasing with time. It influences the heat transfer and hydrodynamic behavior as follows: heat transfer is reduced due to an increase of the coolant side thermal resistance with an increasing layer thickness of carbon deposition. Pressure loss is increased due to roughness elements on the cooling channel wall [10].

Single tube heat exchanger experiments have been accomplished to define certain wall temperature limits for the application of hydrocarbon fuels as coolant. It has been observed that for each fuel, a wide range of maximum acceptable wall temperatures is found. Coking of fuels is dependent on the wall material and coatings such as gold plating, platinum plating, nickel plating and silver plating [10].

2.2.2 Potential chemical reactions with liner material

Corrosion of the liner wall material occurs if the fuel contains a certain part of sulfur. Copper corrosion produces rough wall layers with reduced thermal conductivity and causes an additional pressure loss in the cooling channels [10].

Contamination of sulfur and oxygen in the fuels are responsible for sulfurize and oxidize copper, which results in a deterioration of the copper wall. Carbon deposition from heated hydrocarbon fuels on a hot copper wall can cause copper corrosion [10].

Hydrogen embrittlement is a degradation of mechanical properties, especially in plasticity, of materials relevant for many metallic materials, including steel, aluminum (at high temperatures only), and titanium. High-pressure hydrogen gas, electrochemical hydrogen charging and corrosion reactions are the typical sources of hydrogen embrittlement in metals [11]. Prevention of hydrogen embrittlement can be based on surface coating and surface modification treatments or the modification of the material microstructure [11].

2.2.3 Pressure drop and heat transfer

The physical properties of the coolant are influencing the heat transfer. Good coolants are high density fluids with a high heat capacity c_p and low dynamic viscosity η. A comparison of the heat capacity of different coolants is given in Fig. 4 and of viscosity in Fig. 5 all in the typical operational range of regenerative cooling of high-performance rocket engines.

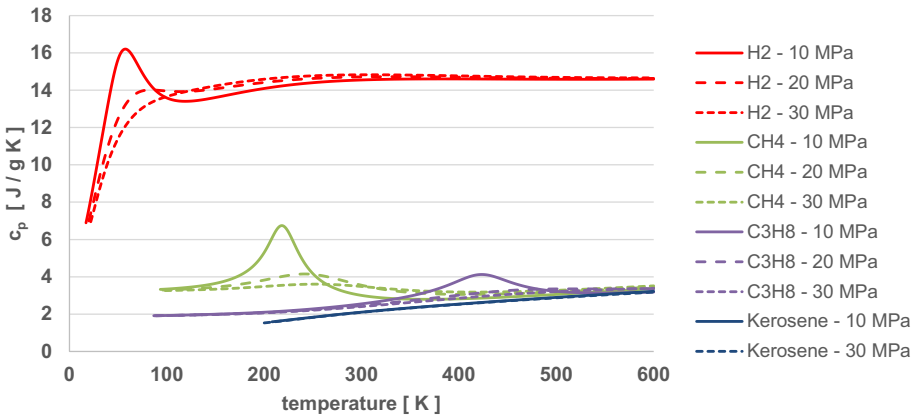

Fig. 4 Heat capacity of selected propellants [10, 12]

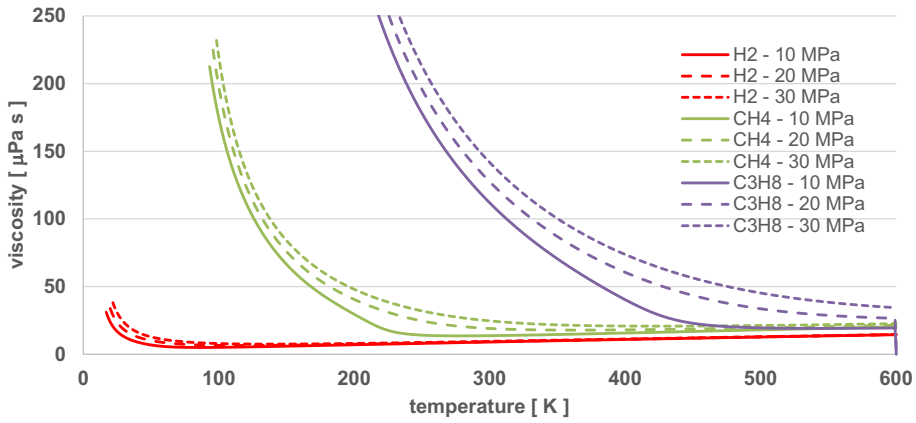

Fig. 5 Viscosity of selected propellants [12]

Table 3 Triple point conditions of cryogenic propellants [12]

	LOX	LH2	LCH4	LC3H8
Triple point temperature [K]	54.361	13.803	90.694	85.525
Tripe point density [kg/m^3]	1306.1	76.977	451.48	733.13
Density increase compared to filling conditions in Table 1	14.4%	8.6%	6.8%	26%

2.3 Key characteristics at triple point

Usually cryogenic propellants are loaded into the tanks at their boiling point under ambient pressure (already shown in Table 1). However, employing colder, subcooled propellants offers the benefit of increased density. Subcooled propellants are currently being used by SpaceX in both their currently operating Falcon 9 rocket as well as the Starship configuration under development.

The maximum density increases possible, while still remaining fully liquid, is given for the cryogenic propellants in Table 3. The increase is especially large for LOX and LC3H8. For RP-1 the lowest possible temperature (as well as properties such as the boiling point) are not easily defined since it is a mixture of various hydrocarbons. However, in principle the RP-1 can also be subcooled in order to increase the density, as is done for the Falcon 9.

While the increased density is beneficial for the structural index and thus performance of the vehicles, it comes at a price. Loading the propellants at boiling point has the benefit of a well-defined state throughout propellant loading. While propellant may evaporate, the body of fluid itself remains at the boiling point with a constant temperature and density. For a subcooled propellant, any heat influx will lead to thermal stratification which has to be well-understood and managed in order to arrive at useful values for the average propellant density (and thus actually loaded propellant mass on the launch pad) and the thermal residuals.

3 Main propulsion rocket engines

Despite the engines being generic, their selected technical characteristics for simulation are strongly oriented towards data of existing types or previous or ongoing development projects, whenever possible.

The two rocket engine cycles most commonly used in first or booster stages are included in the study:

- Gas-Generator-cycle (GG)
- Staged-Combustion cycle (SC).

Expander cycle engines which exclusively use the heat transferred to the fuel in the regenerative circuit to power the turbopumps have *not* been considered. The Japanese LE-9 in the H-3 launcher is the first application of this cycle in first or booster stages [13]. However, the H-3 is an expendable vehicle and the more demanding missions of reusable first stages make expander cycle engines less attractive for this application. DLR has looked in the past into the feasibility of such open expander engines (LOX-LH2) for reusable winged side-mounted boosters. Although, a converging design could be found under certain conditions at the time, its limitations were also revealed with the necessity to implement a vast combustion chamber generating sufficient heat transfer, highly efficient impulse turbines, and significantly larger tanks compared to gas generator cycle configurations because of the relatively low chamber pressure and engine mixture ratio [14, 15].

3.1 Numerical simulation methods

3.1.1 Chamber performance estimation

3.1.1.1 Ideal performance The baseline of all engine performance calculations is the theoretical rocket engine performance estimation for which the following assumptions are made for its calculation:

- adiabatic, isenthalpic combustion;
- adiabatic, isentropic (frictionless and no dissipative losses) quasi one-dimensional nozzle flow;
- ideal gas law;
- no dissipative losses.

This calculation approach for theoretical rocket engine performance is commonly used since decades and has been implemented in the famous NASA "Lewis code" developed in the 1960s by Zeleznik, Sanford Gordon and Bonnie J. McBride [16, 17]. The condition for chemical equilibrium can be stated in the minimization of Gibbs energy or the maximization of entropy. According to the second law of thermodynamics an isolated system is at equilibrium when entropy is constant and reaches its maximum [18, 19].

The analysis is started by obtaining the combustion chamber equilibrium composition assuming the isobaric-isenthalpic combustion, followed by calculation of the thermodynamics derivatives from the equilibrium solution [20]. The results include the number of moles for each species, combustion temperature, heat capacity, enthalpy and entropy of the reacting mixture, as well as specific heat ratio and velocity of sound. The calculation tools implement a thermodynamic analysis module which utilizes a free energy minimization approach to obtain the combustion composition for given propellant components and combustion conditions.

3.1.1.2 Models for non-ideal performance Ideal performance calculations provide an overestimation of actual engine performance. This is on the one hand related to less efficient open cycles that bring propellants to chamber pressure conditions (see following Sect. 3.1.2) and on the other hand is linked to constraints of the gas expansion process relevant for all cycles.

Those factors relevant for the liquid rocket engine predesigns performed here are including:

- non- chemical equilibrium conditions,
- performance loss due to finite-area combustor,
- performance loss due finite rate chemical reaction kinetics,
- nozzle wall friction loss,
- nozzle divergence loss,
- performance change due to nozzle flow separation.

In ideal performance, the composition is assumed to attain its chemical equilibrium instantaneously. While this assumption is a good approximation in the combustion chamber, it is not realistic in rapid supersonic expansion. In "frozen" performance, composition is assumed to remain fixed at a certain combustion composition during expansion [18] and is no longer able transforming chemical into kinetic energy. The early CEC/CEA-codes of NASA offered already the equilibrium and "frozen" performance calculation options with actual performance to be expected in between these upper and lower theoretical limits.

The consideration of finite rate chemical reaction kinetics is important for realistic rocket engine performance estimation. Assuming full chemical equilibrium along the complete nozzle can overestimate the I_{sp} by 10 s or more depending on the expansion ratio [5]. Usually it is recommended in rocket performance assessment that the combustion composition is assumed to remain fixed ("frozen") at certain area- or pressure-ratios during expansion. A classic, however, slightly conservative assumption is "freezing" chemical composition at the nozzle throat. The commercially available rocket engine tool RPA (rocket propulsion analysis) recommends empirically derived values [21] depending on the combustion products at different supersonic area ratios A_{fr}/A_t (where A_{fr} is the cross-section after which chemical composition is assumed frozen):

- LOX–Kerosene (hydrocarbons): 1.3
- LOX–LH2: 3.0

These values are recommendations and the actual input is selected by the user potentially based on specific test data. This study is following the empirically-based data and assumes for the less well-known propellant compositions LOX–LCH4 and LOX–LC3H8 values between 1.9 and 2.

Other factors create additional losses compared to the ideal performance. These might simply be considered by correction factors derived from recalculation of existing engines. Such an approach had been implemented in the ASTOS launcher optimization tool within the ESA-funded CDO-project [22]. A more sophisticated method is used by tools like RPA [23] capable of predicting the delivered performance of a thrust chamber using semi-empirical relations to obtain performance correction factors more specific to engine design parameters.

Practical combustion chambers of large-scale engines have relatively small cross sections with contraction area ratios A_c/A_t of less than four. In this case the expansion of the gases is accompanied by significant acceleration and resulting pressure drop. The acceleration process in the chamber is assumed to be adiabatic, but not isentropic, and the pressure drop leads to the lower pressure at nozzle inlet p_c. This causes a small loss in specific impulse [20] which can be calculated. The iterative procedure for its computation in the so-called Finite Area Combustor is described in [21].

A correction factor that represents performance loss due to finite rate kinetics in the combustion chamber depends on propellant combination, oxidizer excess coefficient and chamber pressure [21].

In real thrust chambers the flow is mostly axisymmetric two-dimensional (or even three-dimensional), with a

viscous boundary layer next to the nozzle walls, where the gas velocities are much lower than the core-stream velocities, finite-rate chemical kinetics, and other factors which further reduce the real delivered performance [21]. The correction factor due to wall friction in boundary layer can be calculated according to the fluid dynamic relations of laminar and turbulent boundary layers.

A theoretical ideal nozzle would expand the flow fully parallel to the centerline. Such nozzles are unpractical for any launcher application and hence the nozzle exit angle $> 0°$ is creating some flow divergence and related performance losses. The correction factor can be calculated depending on the nozzle type, expansion ratio and selected fractional length (see e.g. [21]).

The performance of flow separation inside the nozzle could be estimated by RPA [21]. In steady engine operation such flow separation caused by strong overexpansion should be avoided.

3.1.2 Cycle performance, size and mass estimation

All preliminary engine definitions have been performed by simulation of steady-state operation at 100% nominal thrust level using the DLR-tools *lrp* (liquid rocket propulsion) and *ncc* (nozzle contour calculation program) as well as the commercially available tool *RPA*. Any potential requirements specific to transient operations or deep-throttling are not considered in this early design study.

DLR's lrp-program has a long heritage of early rocket engine pre-sizing based on a selection of fixed internal engine flows combined with a rough estimation of engine size and empirically based mass estimation per major component. The commercially available program RPA (versions 2.2.3 and 2.3.2) [23, 24, 20] has been used as a second tool for crosscheck of results and for improved modelling of certain cycle variants like oxygen-rich preburner systems. The RPA engine cycle analysis module is capable of analyzing the operational characteristics of engine configurations, performing a power balance of the turbomachinery to achieve the defined combustion chamber pressure. RPA offers more sophisticated performance estimation methods [21] and can be operated by graphical user interface or by scripts. In the preliminary definition of the reusable rocket engines, both numerical tools are useful and complement each other.

The program ncc generates the internal thrustchamber contours of different bell-type nozzles based on the main combustion chamber (MCC) operating conditions and definition of characteristics like characteristic chamber length, nozzle fractional length, contraction- and expansion ratio, etc. Further, ncc can create input files for the NASA code TDK [25] allowing conveniently subsequent analysis of boundary layer effects.

3.2 Baseline design assumptions

3.2.1 Programmatic requirements

Reliability and robustness are basic requirements, excluding any exotic technical options. Further, the propulsion system choice should be environmentally compatible with non- or low-toxic propellants and reaction products. This point has been addressed by the four selected propellants described in Sect. 2. Sustainability of space flight gains increasing importance. The life-cycle and climate impact of the propulsion system is a key element for all launchers and should be as low as possible. A quantitative assessment of the different options is going beyond the scope of this paper and should be addressed in future activities.

Development risks should be limited and potential concepts should build upon European expertise in operating engines or technology demonstration performed or ongoing. The propulsion system should, thus, be affordable in development but also later in manufacturing and launcher operations. The target for reusability is set between minimum of 5 to maximum 25 ignitions or flights. A quantified assessment of such high-level programmatic requirements is not pursued in the study.

3.2.2 Technical requirements

3.2.2.1 Thrust level Common baseline assumption of all engines is a vacuum thrust in the 2200 kN-class. This a-priori-choice is keeping future heavy-lift launcher options in mind and is also set by the upgrade limits of European test infrastructure for liquid rocket engines. Most VTVL- and VTHL-launcher configurations described in [2, 3] have a lower thrust requirement. The engine massflows are scaled to the required thrust level of the individual RLV-concepts while I_{sp}-performance and engine thrust-to-weight ratios (T/W) are kept in [2, 3] on the values described below.

3.2.2.2 Chamber pressure In case of the staged-combustion engines, the main combustion chamber (MCC) pressure is commonly fixed for all propellant combinations at 160 bar (16 MPa). This moderate value in Russian or US perspective has been chosen considering the limited European experience in closed cycle high-pressure engines.

The chamber pressure for the gas-generator type is unlikely to be set on the same value of 16 MPa. Figure 6 shows the performance difference of the LOX-LH2 gas generator engine as a function of MCC pressure compared to the reference staged combustion (SC) cycle at 160 bar (16 MPa).. The difference in I_{sp} is shown for sea-level

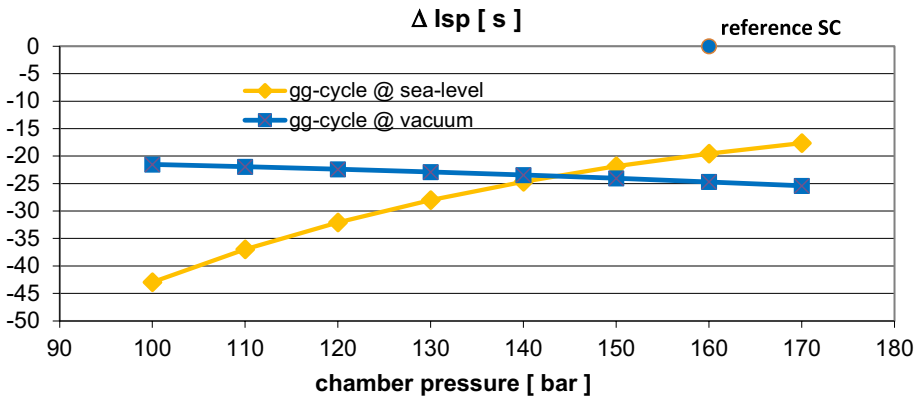

Fig. 6 Trade study on main combustion chamber pressure sensitivity for GG-cycle on I_{sp} performance, sea-level (yellow), vacuum (blue)

(yellow) and vacuum conditions (blue) and typical nozzle expansion ratio of 30. The open cycle's performance is at least 15 to 20 s below the closed cycle but could degrade by 30 to 40 s if parameters are not carefully selected. Raising the main combustion chamber pressure of the open gas generator cycle beyond 100 bar is widening the I_{sp}-gap in vacuum when compared to the reference SC-point while for sea-level conditions the gap closes in. The explanation of this behavior is straight-forward and well known: Increasing the chamber pressure requires swelling the low-efficiency secondary flow powering the turbopumps and, consequently, does no longer allow improving overall engine performance in vacuum. At sea-level, the increased MCC-pressure results in higher nozzle exit pressure and delivers significantly improved performance despite elevated, less-efficient gas generator flow.

Subsequently, the main combustion chamber pressure for the gas-generator type is commonly set to 12 MPa. This pressure is not far from the useful upper limit of this cycle but is assumed necessary to achieve sufficient performance for the RLV stages. Europe has considerable experience in this range with Vulcain 2 operating at 11.7 MPa and the development risk of the additional slight increase is assessed as low.

3.2.2.3 Nozzle expansion ratio Nozzle expansion ratios are selected according to optimum performance but also requirements of safe throttled operations when landing VTVL-stages. For the first stage engines data are calculated for several expansion ratios from 20 for gas generator types up to 35 for the staged-combustion variants. The upper stage engines are derived from the first stage engines with the only difference being the increased nozzle expansion. The impact of this value is evaluated for expansion ratios of 120 and 180.

3.2.2.4 TET and cooling Turbine entry temperature (TET) target is set around 750 K and kept in all cases below 800 K to be compatible with the increased lifetime requirement of reusable rocket engines. These assumptions are in the lower segment of the typical range of rocket engine TET. Reference [5] mentions an elevated range between 900 to 1200 K, however, not having any reusability in focus. The reusable SSME has preburner combustion temperatures of 739 K on the OTP-side and up to 983 K on the FTP-side [33].

Further, for all engines in this study regeneratively cooled combustion chambers supported by film cooling at the wall using small amount of fuel are assumed. Large down-stream nozzle extensions should use a combination of dump- and radiation cooling.

3.2.3 Design assumptions

Beyond the already described technical design requirements, some parameters need to be selected for the engine cycle analyses and engine pre-dimensioning. These are the turbomachinery efficiencies, gas-generator operating pressure and turbine pressure ratio in open cycles and internal line, valve and injector total pressure losses.

The parameters can be preselected and iteratively further optimized during the maturing engine design process. However, such an approach applied to the numerous engine configurations would go well beyond the scope of this study. Instead, typical engine component values have been selected but are not validated by sophisticated analyses. Data are similar within narrow limits but not identical for all types. An open cycle high pressure-ratio impulse turbine can't reach the same efficiency as the low pressure-ratio turbines in closed cycle engines.

The actually selected design parameters of the turbopumps are listed in the following together with the short engine descriptions. In case more elaborated turbomachinery data are available based on dedicated designs, the references are provided. Selection of the parameters within the narrow boundaries has only limited impact on performance

and mass estimation. The driving factors remain propellant combination, cycle and nozzle expansion ratio.

3.3 LOX-LH2 engines

The combination of liquid oxygen with liquid hydrogen delivers the highest practically achievable mass specific performance. Water as the reaction product is also the most environmentally compatible exhaust. The low bulk density due to the low density of hydrogen and its very low boiling temperature are the key challenges.

Europe has gained significant experience with these propellants in more than 50 years and has flown several hundred engines up to date (HM7 from 1979 to 2023 and Vulcain since 1996).

The selection of the engine mixture ratio (MR) has a major impact on overall performance. However, the optimum I_{sp} as shown for example in typical conditions in Fig. 3 is not exactly at the optimum of the launcher. If a new engine is designed for a dedicated launcher application, an iterative MR-optimization could be performed considering tank sizing or trajectory optimization. However, usually the vehicle is not yet well defined when engine MR is to be chosen. Nevertheless, a preliminary choice of the main combustion chamber MR close to the I_{sp}-optimum is recommended with small offset to the right, towards increased propellant density for reduced tank size.

This approach is followed for the hydrocarbon-based types described in the following sections. The case of the LOX-LH2 propellant combination is somehow special because of its low average bulk density as shown in Fig. 2. Therefore, both types have been set a-priori to an engine MR of 6.0 which is a good compromise between performance, acceptable propellant bulk density of the stage, and technical feasibility of the combustion process. This choice of 6.0 is supported by the design of many existing LOX-LH2 main stages which are around this value.

As clearly visible in Fig. 7, the main combustion chamber operating points are off the optimum I_{sp}-performance, shifted to the right towards increased density. In case of the gas generator cycle chamber (blue curve) this shift is more pronounced into less favorable regions (6.77, indicated by red arrow). This shift is necessary in order to reach an engine MR of 6.0 because the turbines are driven by strongly hydrogen-rich hot gas. The closed cycle's MCC MR is, consequently, exactly at the engine mixture ratio of 6.0 because the secondary flow is not disturbing.

3.3.1 Open gas-generator cycle

The architecture of the open cycle is following the conventional approach with single gas generator and two separate turbopumps run in parallel. This is similar to the Vulcain engine and nominal gas generator pressure is selected at 11 MPa. The turbine power-pack data assumptions for the dual shaft design have been selected as follows:

- GG combustion temperature 780 K
- LOX turbine efficiency 48%
- LOX turbine pressure ratio 16.5
- LOX pump efficiency 75%
- LH2 turbine efficiency 53%
- LH2 turbine pressure ratio 16.9
- LH2 pump efficiency 75%

3.3.1.1 First stage engine performance assessment Based on these assumptions and the 2200 kN vacuum thrust requirement, three reference engines have been calculated with different nozzle expansion ratios (Table 4), all of potential interest for the RLV first stage application.

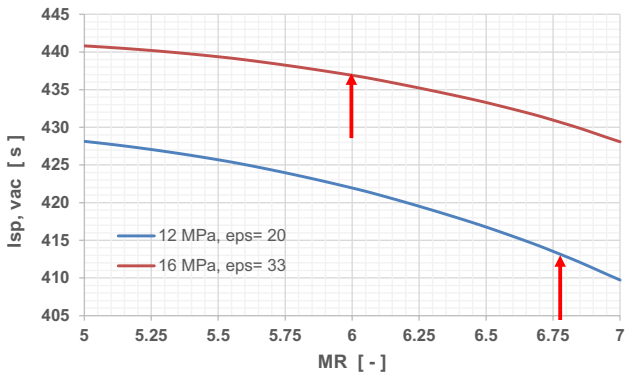

Fig. 7 Influence of LOX/LH2-mass ratio in main combustion chamber on $I_{sp,vac}$ chamber performance (red arrows indicating selected MCC design points)

Table 4 Performance data of LOX-LH2 gas generator cycle engines from lrp1.1 calculation

Nozzle expansion ratio	–	20	30	35
Sea level thrust	kN	1990.9	1893.6	1845.5
Vacuum thrust	kN	2200	2200	2200
Sea level spec. impulse	s	366.9	357.2	351
Vacuum spec. impulse	s	405.4	415	418.4
Chamber pressure	bar	120	120	120
Total engine mass flow	kg/s	553.3	540.45	536.11
gg mass flow	kg/s	20.9	20.4	20.2
Total engine mixture ratio	–	6	6	6
Chamber mixture ratio	–	6.77	6.77	6.77
Nozzle exit pressure	bar	0.7	0.412	0.34

Comparing the calculation methods in Table 4 with a computation using RPA of the engine with expansion ratio 20 shows a difference in I_{sp} performance at vacuum condition of less than 1.3 s (0.3%) and 4.5 s at sea-level (1.28%). These numbers give an indication on the level of uncertainty in the numerical performance calculation.

Another comparison of calculated performance with real operating engines is most suitable for the RS-68 which has been designed for a similar launcher application in Delta IV main and booster stage and which also has a relatively low expansion ratio. The calculated engine performance data of variant $\varepsilon = 20$ is found slightly below those published for the RS-68. The American engine has a slightly lower combustion pressure of 11.26 MPa while nozzle expansion is at 21.5. The vacuum I_{sp} is announced to reach 409 s [26]. The very large size of the RS-68 (2950 kN) with related potential efficiency gains should be taken into account in the comparison as well as uncertainty of its TET.

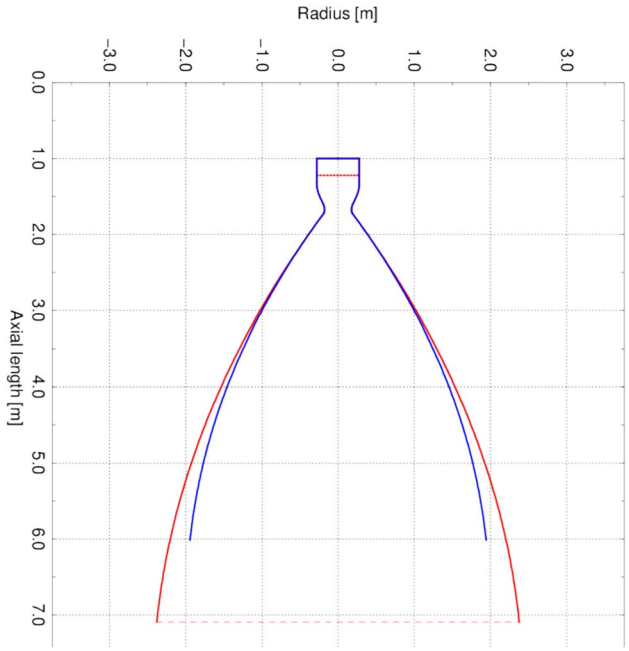

Fig. 8 Thrust chamber internal contours of LOX/LH2 GG-engine with nozzle expansion ratio 180 (red) and 120 (blue)

3.3.1.2 Upper stage engine derivative Using the same core engine in the upper stage in order to save cost is one of the baseline design drivers of the ENTRAIN TSTO configurations. Therefore, two upper stage engines with significantly increased nozzle expansion ratios of 120 and 180 have been defined using the $\varepsilon = 20$ design. Calculated engine performance is listed in Table 5. For the same mass flow, vacuum thrust increases by up to 10%. Items not listed are identical to the first stage engine. Note the gas generator conditions have not been changed for this calculation. A variation might offer the potential of slight improvements.

3.3.1.3 Engine size and mass The upper stage engines' thrustchambers have further been modeled using the tool ncc assuming parabolic nozzles with 66% fractional length. A sketch of the contours is visible in Fig. 8. Note the enormous size of the engines with a total length of beyond 7 m and exit diameter slightly below 5 m for the $\varepsilon = 180$ variant.

However, at the current state of investigations it is not possible to confirm that such a design is actually achievable. Anything similar has never been realized in the past and a launcher design based on a large upper stage engine having an expansion ratio of 180 would be subject to major development risk. In subsequent steps of the investigations, it has been decided to restrict the upper stage engine to an expansion ratio of 120.

The following rough geometry and mass data (Table 6) have been calculated using the tool lrp1.1.

Table 5 Performance data of LOX-LH2 gas generator cycle upper stage engines from lrp1.1 calculation

nozzle expansion ratio	–	120	180
vacuum thrust	kN	2389	2420
vacuum spec. impulse	s	440.4	446

3.3.2 Closed staged-combustion cycle

The staged combustion cycle reference engine is derived of the SLME (SpaceLiner Main Engine) under investigation for several years at DLR (e.g. [27–31]). A full-flow staged combustion cycle (FFSC) with fuel-rich preburner gas driving the LH2-pump and oxidizer-rich preburner gas driving the LOX-pump is a preferred design solution for the SLME.

In a full-flow staged combustion cycle the complete fuel and oxidizer flow rates are fed through one of the preburners after being pressurised by each turbo pump. Subsequently, the turbine gases are all injected in hot gaseous condition into the main combustion chamber (MCC).

The operational domain of the SLME has been preliminarily defined [30, 31]: The SLME in the SpaceLiner application is operating at MR = 6.5 during lift-off and is later throttled to MR = 5.5 by reducing the LOX-massflow. The intermediate SLME operating point O1 with a mixture ratio of 6 is typical for LOX-LH2 engines and with its moderate 16 MPa chamber pressure is used as the reference condition for the RLV-ENTRAIN-system studies.

The turbine power-pack data assumptions for the dual preburner, integrated powerhead design have been selected based on preliminary component sizing in [31]:

Table 6 Geometry and mass data of LOX-LH2 gas generator cycle engines

Nozzle expansion ratio	–	20	30	35	120	180
Total engine length	m	2.76	3.25	3.47	6.18	7.47
Nozzle exit diameter	m	1.62	1.96	2.11	3.97	4.86
Total engine mass	kg	2275.54	2287.18	2300.56	2955.9	3378.2
T_{vac}/W	–	98.55	98	97.48	82.4	73

Table 7 Performance data of LOX-LH2 staged combustion cycle engines from lrp1.1 calculation

Nozzle expansion ratio	–	23	33	35
Sea level thrust	kN	2024.3	1952.5	1938.2
Vacuum thrust	kN	2200	2200	2200
Sea level spec. impulse	s	394	387	385
Vacuum spec. impulse	s	428	436. 5	437.8
Chamber pressure	bar	160	160	160
Total engine mass flow	kg/s	523.3	513.8	512.3
Engine mixture ratio	–	6	6	6
Nozzle exit pressure	bar	0.705	0.438	0.405
Power Pack conditions:				
Ox-rich preburner MR	–	≈ 130	≈ 130	≈ 130
Ox-rich preburner pressure	bar	262.9	262.9	262.9
Ox-rich preburner massflow	kg/s	408.7	401.2	400.1
Fuel-rich preburner MR	–	≈ 0.6	≈ 0.6	≈ 0.6
Fuel-rich preburner pressure	bar	266.2	266.2	266.2
Fuel-rich preburner massflow	kg/s	114.6	112.5	112.2

- Ox-rich preburner combustion temperature 775 K
- LOX turbine efficiency 87%
- LOX pump efficiency 86%
- Fuel-rich preburner combustion temperature 769 K
- LH2 turbine efficiency 92%
- LH2 pump efficiency 79%

N.B.: calculated performance of all closed cycles is independent of the internal architecture. Thus, a fuel-rich preburner variant like the one used in the SSME (space shuttle main engine) or proposed for the European SCORE-D demonstrator [32] would achieve the same I_{sp} as a Full-Flow-cycle engine. The difference is in engine complexity and has an impact on mass.

3.3.2.1 First stage engine performance assessment The requirements of the ENTRAIN study with tandem arrangement of stages (see [2, 3]) are not identical to the SpaceLiner and therefore the baseline SLME had been adapted in its nozzle expansion ratio and was recalculated. Based on these assumptions and the 2200 kN vacuum thrust requirement, three reference engines have been calculated with different nozzle expansion ratios (see Table 7), all of potential interest for the RLV first stage application.

Table 8 Performance data of LOX-LH2 staged combustion cycle upper stage engines from lrp1.1 calculation

Nozzle expansion ratio	–	120	180
Vacuum thrust	kN	2317	2343
Vacuum spec. impulse	s	458.6	463

A comparison of calculated performance with real operating engines is suitable for the SSME (RS-25), originally been designed for the Space Shuttle and now used in the core stage of SLS. The SSME expansion ratio is 69 and achieves a vacuum I_{sp} of 452 s when operating at 109% thrust level with 21 MPa chamber pressure [33].

3.3.2.2 Upper stage engine derivative Following the ENTRAIN TSTO propulsion logic, two similar upper stage engines with significantly increased nozzle expansion ratio of 120 and 180 have been defined using the $\varepsilon = 33$ design. Calculated engine performance is listed in Table 8. For the same mass flow, vacuum thrust increases by about 6.2%. Items not listed are identical to the first stage engine.

3.3.2.3 Engine size and mass Rough geometry and mass data have been calculated using the tool lrp1.1 and are listed in Table 9. As all 1st-stage engines are scaled for 2200 kN vacuum thrust, the variant with larger expansion ratio has a slightly reduced mass flow and hence reduced throat diameter (approximately 3 mm difference or 1%).

T_{vac}/W is calculated approximately 24% below the gas generator cycle, however, under different assumptions in chamber pressure and nozzle expansion ratio. The explanation is mainly found in the more powerful and heavier turbopumps and the two high-pressure preburners.

3.4 LOX-RP1 engines

The combination of liquid oxygen with kerosene is by far the most commonly used propellant combination in spaceflight. Still today LOX-RP1 is the fuel choice of more than 50% of all rockets flown worldwide.

The spaceflight heritage of LOX-RP1 is impressing:

- Launching the first artificial satellite (R-7 rocket (8K71PS)),

Table 9 Geometry and mass data of LOX-LH2 staged combustion cycle engines

Nozzle expansion ratio	–	23	33	35	120	180
Total engine length	m	2.55	2.92	2.98	5	6
Nozzle exit diameter	m	1.49	1.77	1.82	3.37	4.12
Total engine mass	kg	3006	2992	2991	3362.2	3617.5
T_{vac}/W	–	74.6	74.9	74.95	70.2	66

- Launching the first man to space (R-7 rocket (8K72K)),
- Launching the first man to the Moon (S-IC first stage with F1-engine on Saturn V rocket),
- Achieving the highest operational chamber pressure (RD-180 engine on Atlas V),
- Powering the first operational RLV-booster stage (Merlin 1D engine on Falcon 9).

Early European experience exists with the British Blue Streak but was discontinued with the demise of the Europa rocket in the early 1970s.

The strategy in selecting combustion chamber operating points is different for hydrocarbon engines than for hydrogen engines. The reason is the increased sensitivity of I_{sp} to MR variations (see Fig. 3) in contrast to hydrogen, where the dependence is rather flat. Figure 9 shows the selected main combustion chamber operating points (red arrows) close to the optimum performance, slightly shifted to the right towards increased density. In case of the gas generator cycle (blue curve) this shift is a bit more pronounced into less favorable regions (2.66) because the turbines are driven by strongly fuel-rich hot gas. This choice helps avoiding the engine and hence tank mixture ratio dropping below 2.2. The closed cycle's MCC MR is exactly at the engine MR of 2.6.

Note, engine mixture ratio of the hydrogen engines had been set independent of the cycle to 6.0 (see Sect. 3.3) to keep average propellant density acceptable for the vehicle design. For all hydrocarbon engines the propellant density is less a concern and instead performance becomes more important. Therefore, the chamber operating points are selected not far from the individual optimums.

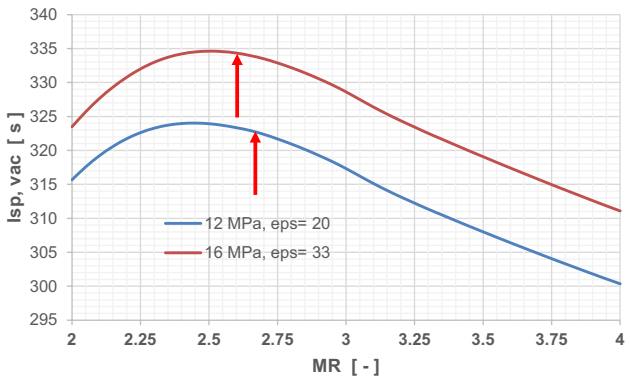

Fig. 9 Influence of LOX/RP1- mass ratio in main combustion chamber on $I_{sp,vac}$ chamber performance (red arrows indicating selected MCC design points)

Table 10 Performance data of LOX-RP1 gas generator cycle engines from lrp1.1 calculation

Nozzle expansion ratio	–	20	30	35
Sea level thrust	kN	1984	1884	1834
Vacuum thrust	kN	2200	2200	2200
Sea level spec. impulse	s	279	272	267
Vacuum spec. impulse	s	310	317	320
Chamber pressure	bar	120	120	120
Total engine mass flow	kg/s	723.4	706.1	700.3
gg mass flow	kg/s	47.2	46	45.7
Total engine mixture ratio	–	2.25	2.25	2.25
Chamber mixture ratio	–	2.66	2.66	2.66
Nozzle exit pressure	bar	0.72	0.42	0.34

3.4.1 Open gas-generator cycle

The architecture of the open cycle is following the typical approach with single gas generator and single shaft turbopump. This is similar to many famous gas-generator cycle RP1-engines like F1 or Merlin 1D. The nominal gas generator pressure is selected at 11 MPa. The turbine power-pack data assumptions have been selected as follows:

- GG combustion temperature 780 K
- turbine efficiency 50%
- turbine pressure ratio 16.5
- LOX pump efficiency 75%
- RP1 pump efficiency 75%

3.4.1.1 First stage engine performance assessment Based on these assumptions and the 2200 kN vacuum thrust requirement, three reference engines have been calculated with different nozzle expansion ratios (Table 10), all of potential interest for the RLV first stage application.

Another performance calculation has been executed for the engine with expansion ratio 20 by using the cycle analysis tool RPA 2.23 under identical assumptions. Comparing the two calculation methods shows a difference in I_{sp}

performance at vacuum condition of less than 1.3 s (0.3%) and 4.5 s at sea-level (1.28%).

A comparison of calculated performance with real operating engines is most suitable for the SpaceX Merlin 1D which has been designed for a similar launcher application in Falcon9 main- and with increased nozzle expansion ratio in the upper stage. The calculated engine performance of the engine with nozzle area ratio 20 is found very similar to data published for the Merlin 1D. Although chamber pressure of the latest and most powerful Merlin 1D + is not exactly known, under considerations for the thrustchamber geometry and published thrust level of the -1D, a combustion chamber pressure of 12 MPa is realistic. The 1D + ' vacuum I_{sp} is announced to reach 311 s. In combination with nozzle expansion of 16, the Merlin would show a slightly better performance than the ENTRAIN engine. However, missing information on the turbopump system of Merlin makes the exact comparison difficult.

3.4.1.2 Upper stage engine derivatives Upper stage engines with significantly increased nozzle expansion ratios of 120 and 180 have been defined using the $\varepsilon = 20$ design. Calculated engine performances are listed in Table 11. For the same mass flow, vacuum thrust increases by up to 10%. Note the gas generator conditions have not been changed for this calculation. A variation might offer the potential of slight improvement.

3.4.1.3 Engine size and mass For the gas generator engines rough geometry and mass data (Table 12) have been calculated using the tool lrp1.1. Note the calculated high T_{vac}/W ratios of above 100 for the lower stage engines, still below what is claimed by SpaceX for its Merlin 1D.

Table 11 Performance data of LOX-RRP1 gas generator cycle upper stage engines from lrp1.1 calculation

Nozzle expansion ratio	–	120	180
Vacuum thrust	kN	2397	2430
Vacuum spec. impulse	s	338	342

In subsequent launcher system investigation, it has been decided again to restrict the upper stage engine to an expansion ratio of 120 because of the enormous size of the larger variant with $\varepsilon = 180$ would be subject to major development risk.

3.4.2 Closed staged-combustion cycle

The staged combustion cycle is derived of the NPO Energomash RD-120 (11D123) with oxidizer-rich preburner. In case of hydrocarbon staged combustion cycle engines, the oxygen-rich pre-combustion allows for significantly lower turbine pressure ratios compared to fuel-rich preburners in otherwise similar engine architectures [34]. The driving factor is the product of specific enthalpy and turbine gas massflow which is higher for oxygen-rich gas. All Russian closed cycle RP1-engines of the last 50 years are following this design approach.

The power-pack conditions have been selected as follows:

- Ox-rich preburner combustion temperature 750 K
- LOX turbine efficiency 75%
- LOX pump efficiency 75%
- RP1 pump efficiency 75%

Table 13 Performance data of LOX-RP1 staged combustion cycle engines from lrp1.1 and RPA 2.3 calculations

Nozzle expansion ratio	–	23	33
Sea level thrust	kN	2021	1948
Vacuum thrust	kN	2200	2200
Sea level spec. impulse	s	301	296
Vacuum spec. impulse	s	327.7	334.3
Chamber pressure	bar	160	160
Total engine mass flow	kg/s	684.55	670.95
Engine mixture ratio	–	2.6	2.6
Nozzle exit pressure	bar	0.77	0.48
Power Pack conditions:			
Ox-rich preburner MR	–	≈ 51.4	≈ 51.4
Ox-rich preburner pressure	bar	314.9	314.9
Ox-rich preburner massflow	kg/s	504.1	494.1

Table 12 Geometry data of LOX-RP1 gas generator cycle engines from lrp1.1 calculation

Nozzle expansion ratio	–	20	30	35	120	180
Total engine length	m	2.93	3.45	3.67	6.5	7.85
Nozzle exit diameter	m	1.65	1.99	2.14	4.03	4.94
Total engine mass	kg	1978	1982	2016	2716	3175
T_{vac}/W	–	113.4	112.2	111.2	89.9	78

3.4.2.1 First stage engine performance assessment Based on the same 2200 kN vacuum thrust requirement as for LOX-LH2, two reference engines have been calculated with different nozzle expansion ratios (see Table 13), both of potential interest for the RLV first stage application. RPA is capable of calculating an oxygen-rich preburner staged combustion cycle. Overall engine performance estimated by RPA is found very close to lrp1.1 results with largest deviations again in sea-level conditions. Relative difference here is less than 0.53% while in vacuum the relative difference is less than 0.006% (0.02 s).

3.4.2.2 Upper stage engine derivative Similar to the previous sections, upper stage engines with significantly increased nozzle expansion ratios have been defined using the $\varepsilon = 33$ first stage configuration for area ratio 180 and a smaller one with $\varepsilon = 120$. Calculated engine performance is listed in Table 14. For the same mass flow, vacuum thrust increases by up to 7%. Items not listed are identical to the first stage engine.

The Russian upper stage engine RD-120 (11D123) by NPO Energomash has a similar chamber pressure of 16.28 MPa and an oxygen-rich preburner architecture. The calculated specific impulse of the smaller engine with $\varepsilon = 120$ is close to the vacuum I_{sp} of RD-120 of 350 s which has a slightly smaller nozzle expansion ratio of 114.5 [35].

3.4.2.3 Engine size and mass Calculated geometry and mass data of the staged combustion engines are listed in Table 15. As the first stage engines are scaled for 2200 kN vacuum thrust, the variant with larger expansion ratio has a slightly reduced mass flow and hence reduced throat diameter. The staged combustion engines are more compact despite the increased expansion ratios due to the higher nominal chamber pressure.

T_{vac}/W is calculated approximately 30% below the gas generator cycle, however, with different assumptions in chamber pressure and nozzle expansion ratio. The explanation is again related in the more powerful and heavier turbopumps and the high-pressure preburner. T_{vac}/W of the variant with expansion 33 is slightly above the engine with expansion 23 because of the latter's slightly larger massflow and hence size of major components.

Table 14 Performance data of LOX-RP1 staged combustion cycle upper stage engine from lrp1.1 calculation

Nozzle expansion ratio	–	120	180
Vacuum thrust	kN	2323	2350
Vacuum spec. impulse	s	353	357

Table 15 Geometry data of LOX-RP1 staged combustion cycle engines

Nozzle expansion ratio	–	**23**	**33**	**120**	**180**
Total engine length	m	2.6	3	4.87	6.57
Nozzle exit diameter	m	1.50	1.78	3.4	4.15
Total engine mass	kg	2825	2809	3179	3602
T_{vac}/W	–	79.3	79.8	74.5	66.6

3.5 LOX-LCH4 engines

Several initiatives are currently working on engines with the propellant combination LOX-Methane. Although proposed several times in the past, this "softly cryogenic" blend has only recently in July 2023 been realized in an operational Chinese small launcher: ZQ-2 of LandSpace [36]. On the other end of the spectrum, SpaceX is developing its Super-Heavy & Starship with increasing success.

N.B.: all calculations are carried out for pure Methane as a fuel, which however is costly to produce. Depending on the available blend, LOX-LNG might be acceptable as a substitute with almost similar performance. Sulfur included in the natural gas from some sources needs to be removed before its liquefied state LNG can be used as a rocket fuel. In this case a clear standard definition of composition is required as it has been defined for kerosene as RP1 in the US or RG1 in Russia.

The main combustion chamber mixture ratios of the LOX-LCH4 combination have been selected close to their optimum I_{sp} (indicated by red arrows in Fig. 10), however, slightly shifted towards increased MR to reach increased bulk density. This approach is the same as for all hydrocarbon engines (see previous Sect. 3.4) and different to the one used for LOX-LH2 engines.

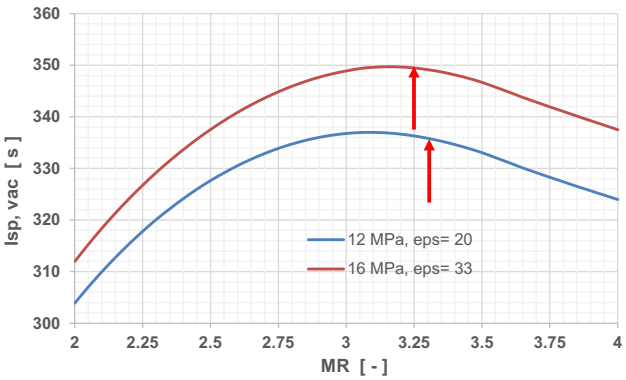

Fig. 10 Influence of LOX/LCH4- mass ratio in main combustion chamber on $I_{sp,vac}$ chamber performance (red arrows indicating selected MCC design points)

The selected MCC-MR of the gas generator engine is 3.3 while MCC-MR in case of the staged combustion thrust-chamber is set to 3.25.

3.5.1 Open gas-generator cycle

The gas generator operates methane-rich and its hot gas powers the single shaft turbine. Major characteristics are derived of the PROMETHEUS-Demonstrator [37] but the baseline assumptions remain similar to all other engines of the system study. The nominal gas generator pressure is selected at 11 MPa. The turbine power-pack data assumptions for the single shaft design have been selected as follows:

- GG combustion temperature 780 K
- turbine efficiency 50%
- turbine pressure ratio 16.5
- LOX pump efficiency 75%
- CH4 pump efficiency 75%

3.5.1.1 First stage engine performance assessment Based on these assumptions and the 2200 kN vacuum thrust requirement, three reference engines have been calculated with different nozzle expansion ratios (Table 16), all of potential interest for the RLV first stage application.

Another performance calculation has been executed for the smaller engine with expansion ratio 20 by using the cycle analysis tool RPA 2.23. Baseline assumptions are mostly identical to the lrp-calculations but the internal iteration process is different. Inducer efficiencies are assumed at only 70% (no separate value in lrp1.1) while turbine efficiency is raised to 54%. Comparing the two calculation methods shows a difference in I_{sp} performance at vacuum condition of 0.0 s (0.0%) and 0.8 s at sea-level (0.28%).

PROMETHEUS is a European engine under development with potential future application in first and upper stages [37]. The characteristics of the engine with nozzle area ratio 20 are in comparable range as the engine should see similar applications. The similar Chinese TQ-12A [36] is operational and its announced sea-level I_{sp} almost exactly fits the performance of the gas generator engine with smallest nozzle in Table 16 (difference < 0.14%).

3.5.1.2 Upper stage engine derivative Upper stage engines with significantly increased nozzle expansion ratios of 120 and 180 have again been defined using the $\varepsilon = 20$ design. Calculated engine performances are listed in Table 17. For the same mass flow, vacuum thrust increases by up to 10.2%. Note the gas generator conditions have not been changed for this calculation. A variation might offer the potential of slight improvement.

3.5.1.3 Engine size and mass Geometry and mass data (Table 18) have been estimated using the tool lrp1.1. As all first stage engines are scaled for 2200 kN vacuum thrust, the variant with larger expansion ratio has a slightly reduced mass flow and hence reduced throat diameter. Note their high calculated T_{vac}/W ratios a little above 100, slightly below the LOX-RP1-engines. Note the enormous size of the engine with $\varepsilon = 180$, reaching a total length of almost 8 m and exit diameter slightly below 5 m. This is another example why such huge size upper stage engines are hardly feasible and in subsequent steps of the study the upper stage engines are restricted to an expansion ratio of 120.

3.5.2 Closed staged-combustion cycle

The staged combustion type is based on an oxidizer-rich preburner design with a single-shaft turbopump. The power-pack conditions have been selected as follows:

- Ox-rich preburner combustion temperature 750 K
- Turbine efficiency 75%
- LOX pump efficiency 79%
- CH4 pump efficiency 78%

3.5.2.1 First stage engine performance assessment Based on the same 2200 kN vacuum thrust requirement as for LOX-LH2, two reference engines have been calculated with different nozzle expansion ratios, both of potential interest

Table 16 Performance data of LOX-LCH4 gas generator cycle engines from lrp1.1 calculation

Nozzle expansion ratio	–	20	30	35
Sea level thrust	kN	1984	1884	1834
Vacuum thrust	kN	2200	2200	2200
Sea level spec. impulse	s	289	281	276
Vacuum spec. impulse	s	320	328	331
Chamber pressure	bar	120	120	120
Total engine mass flow	kg/s	699.4	683.4	677.8
gg mass flow	kg/s	65.8	64.3	63.8
Total engine mixture ratio	–	2.5	2.5	2.5
Chamber mixture ratio	–	3.3	3.3	3.3
Nozzle exit pressure	bar	0.7	0.4	0.34

Table 17 Performance data of LOX-LCH4 gas generator cycle upper stage engines from lrp1.1 calculation

Nozzle expansion ratio	–	120	180
Vacuum thrust	kN	2394	2425
Vacuum spec. impulse	s	348	353

Table 18 Geometry and mass data of LOX-LCH4 gas generator cycle engines

Nozzle expansion ratio	–	20	30	35	120	180
Total engine length	m	2.98	3.49	3.72	6.54	7.89
Nozzle exit diameter	m	1.65	1.99	2.14	4.03	4.94
Total engine mass	kg	2126	2144	2161	2862	3319
T_{vac}/W	–	105	104	103	85.2	74.4

Table 19 Performance data of LOX-LCH4 staged combustion cycle engines from lrp1.1 and RPA 2.3 calculations

Nozzle expansion ratio	–	23	33
Sea level thrust	kN	2016	1950
Vacuum thrust	kN	2200	2200
Sea level spec. impulse	s	314	308
Vacuum spec. impulse	s	342.5	349
Chamber pressure	bar	160	160
Total engine mass flow	kg/s	654.5	641.9
Engine mixture ratio	–	3.25	3.25
Nozzle exit pressure	bar	0.76	0.47
Power Pack conditions:			
Ox-rich preburner MR	–	58	58
Ox-rich preburner pressure	bar	320	320
Ox-rich preburner massflow	kg/s	509.1	499.3

for the RLV first stage application. Additional cycle performance analyses were run using RPA with overall engine performance found close to the lrp1.1 results. Relative difference in sea-level conditions is less than 0.01% (0.25 s) while in vacuum the relative difference is less than 0.55% (1.9 s). Data presented in Table 19 are a combination of both tools' results.

The best comparison to an existing LOX-LCH4 staged combustion engine is probably the SpaceX Raptor. Raptor is operating in Full-Flow Staged Combustion-cycle (FFSC) similar to the SLME (see previous Sect. 3.3.2). The Raptor's sea-level or booster stage version has a nozzle expansion ratio of 34.34 close to the ENTRAIN reference engine but with a significantly higher chamber pressure of at least 250 bar and 300 bar in the latest Raptor variant 2 [38]. This explains the vacuum I_{sp}-values coming close while the sea-level I_{sp} of the ENTRAIN-reference being approximately 20 s below calculated Raptor (351.5 s / 328.7 s) [38] due to its relatively low nozzle exit pressure.

3.5.2.2 Upper stage engine derivative Similar to the previous ENTRAIN designs, upper stage engines with significantly increased nozzle expansion ratios have been defined using the $\varepsilon = 33$ first stage configuration. Calculated engine performance with nozzle area ratios 180 and 120 are listed in Table 20. For the same mass flow, vacuum thrust increases by up to 7%. Items not listed are identical to the first stage engine.

Table 20 Performance data of LOX-LCH4 staged combustion cycle upper stage engine from lrp1.1 calculation

Nozzle expansion ratio	–	120	180
Vacuum thrust	kN	2323	2353
Vacuum spec. impulse	s	366	371

Table 21 Geometry data of LOX-LCH4 staged combustion cycle engines

Nozzle expansion ratio	–	23	33	120	180
Total engine length	m	2.58	2.99	5.39	6.52
Nozzle exit diameter	m	1.49	1.77	3.38	4.14
Total engine mass	kg	2925	2908	3350	3673
T_{vac}/W	–	76.6	77.1	70.6	65.2

3.5.2.3 Engine size and mass The geometry and mass data listed in Table 21 have been calculated using the tool lrp1.1. The staged combustion engines are more compact despite the increased expansion ratios in the first stage application due to the higher nominal chamber pressure.

3.6 LOX-LC3H8 engines

The propellant combination of oxygen with propane has not yet been applied in the launcher sector. Characteristic specific impulse data is close to kerosene and methane, almost in the middle between both. Propane is also a "soft" cryogenic fuel, being in gaseous state under ambient conditions. Propane offers a higher bulk density compared to methane and its potential for densification was identified to be higher than that of methane (see Sect. 2.3, Table 3 and reference [39]).

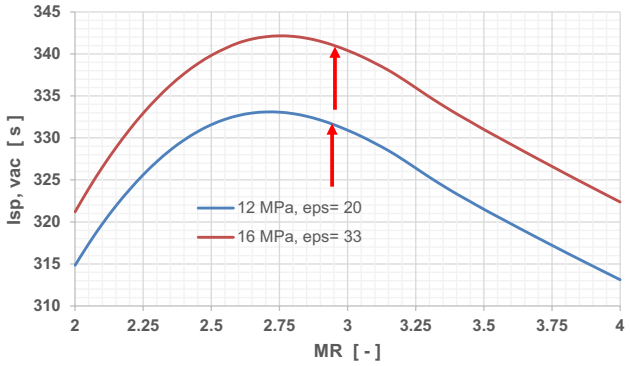

Fig. 11 Influence of LOX/LC3H8- mass ratio in main combustion chamber on $I_{sp,vac}$ chamber performance (red arrows indicating selected MCC design points)

Table 22 Performance data of LOX-LC3H8 gas generator cycle engines from lrp1.1 calculation

Nozzle expansion ratio	–	20	30
Sea level thrust	kN	1984	1884
Vacuum thrust	kN	2200	2200
Sea level spec. impulse	s	284	277
Vacuum spec. impulse	s	315	323
Chamber pressure	bar	120	120
Total engine mass flow	kg/s	710.8	693.8
gg mass flow	kg/s	46.4	45.3
Total engine mixture ratio	–	2.45	2.45
Chamber mixture ratio	–	2.93	2.93
Nozzle exit pressure	bar	0.72	0.42

The process for the selection of operational MR is the same as for the other hydrocarbon engines with MCC-MRs chosen at 2.95 and 2.93 close to their optimum I_{sp} as indicated by red arrows in Fig. 11.

3.6.1 Open gas-generator cycle

The gas generator operates propane-rich and its hot gas powers the single shaft turbopump. Major characteristics remain similar to the baseline assumptions to all other engines of the system study. The nominal gas generator pressure is selected at 11 MPa. The turbine power-pack data assumptions for the single shaft design have been selected as follows:

- GG combustion temperature 780 K
- turbine efficiency 50%
- turbine pressure ratio 16.5
- LOX pump efficiency 75%
- C3H8 pump efficiency 75%

Table 23 Performance data of LOX-LC3H8 gas generator cycle upper stage engine from lrp1.1 calculation

Nozzle expansion ratio	–	120	180
Vacuum thrust	kN	2398	2431
Vacuum spec. impulse	s	344	348

Table 24 Geometry and mass data of LOX-LC3H8 gas generator cycle engines

Nozzle expansion ratio	–	20	30	120	180
Total engine length	m	2.98	3.49	6.54	7.89
Nozzle exit diameter	m	1.64	1.99	4.03	4.93
Total engine mass	kg	2014	2034	2751	3208
T_{vac}/W	–	111.3	110.3	88.8	77.2

3.6.1.1 First stage engine performance assessment Based on these assumptions and the 2200 kN vacuum thrust requirement, two reference engines have been calculated with different nozzle expansion ratios (Table 22), both of potential interest for the RLV first stage application.

Another performance calculation has been executed for the smaller engine with expansion ratio 20 by using the cycle analysis tool RPA 2.32. Baseline assumptions are mostly identical to the lrp-calculations but the internal iteration process is different. Comparing the two calculation methods shows a difference in I_{sp} performance at vacuum condition of 0.54 s (0.18%) and 1.05 s at sea-level (0.37%).

The mini-launcher Spectrum currently under development at Isar Aerospace should use propane as fuel in both of its stages. The Aquila is a gas generator type engine using the LOX-LC3H8 combination and its expansion ratio is around 20. Very little information is available in the public on Aquila and, therefore, no performance comparison can be included here.

3.6.1.2 Upper stage engine derivative Upper stage engines with significantly increased nozzle expansion ratios of 120 and 180 have again been defined using the $\varepsilon = 20$ design. Calculated engine performances are found in Table 23. For the same mass flow, vacuum thrust increases by about 10%. Items not listed are identical to the first stage engine. Note the gas generator conditions have not been changed for this calculation. A variation might offer the potential of slight improvement.

3.6.1.3 Engine size and mass Estimated geometry and mass data of the gas generator engines are listed in Table 24. Note also here the enormous size of the engine with expansion ratio of 180 reaching a total length of almost 8 m and exit

diameter slightly below 5 m. Further note the high calculated T_{vac}/W ratios of slightly above 110.

3.6.2 Closed staged-combustion cycle

The staged combustion type is based on an oxidizer-rich preburner design with a single-shaft turbopump.

The power-pack conditions have been selected as follows:

- Ox-rich preburner combustion temperature 750 K
- Turbine efficiency 75%
- LOX pump efficiency 75%
- C3H8 pump efficiency 75%

3.6.2.1 First stage engine performance assessment Based on similar assumptions as for all staged combustion cycles and the 2200 kN vacuum thrust requirement, two reference engines have been calculated with different nozzle expansion ratios (see Table 25), both of potential interest for the RLV first stage application.

Additional cycle performance analyses using RPA are found close to lrp1.1 results with largest deviations again in sea-level conditions. Relative difference is 3.1 s or less than 1.1% while in vacuum the relative difference is less than 0.5% (1.5 s).

No comparison to an existing LOX-LC3H8 staged combustion engine is available because this propellant-cycle combination has not yet been realized.

3.6.2.2 Upper stage engine derivative Upper stage engines with significantly increased nozzle expansion ratios have been defined using the $\varepsilon = 33$ first stage configuration. Calculated engine performance data of nozzle area ratio 180 and 120 are listed in Table 26. For the same mass flow, vacuum thrust increases by up to 7.1%. Items not listed are identical to the first stage engine.

Table 25 Performance data of LOX-LC3H8 staged combustion cycle engines from lrp1.1 and RPA 2.3 calculations

Nozzle expansion ratio	–	23	33
Sea level thrust	kN	2023	1952
Vacuum thrust	kN	2200	2200
Sea level spec. impulse	s	308	303
Vacuum spec. impulse	s	335	342
Chamber pressure	bar	160	160
Total engine mass flow	kg/s	668.7	668.7
Engine mixture ratio	–	2.95	2.95
Nozzle exit pressure	bar	0.8	0.5
Power Pack conditions:			
Ox-rich preburner MR	–	≈ 54.2	≈ 54.2
Ox-rich preburner pressure	bar	313.9	313.9
Ox-rich preburner massflow	kg/s	500.388	500.388

Table 26 Performance data of LOX-LC3H8 staged combustion cycle upper stage engine from lrp1.1 calculation

Nozzle expansion ratio	–	120	180
Vacuum thrust	kN	2327	2358
Vacuum spec. impulse	s	362	367

3.6.2.3 Engine size and mass Preliminary geometry and mass data (Table 27) have been estimated using the tool lrp1.1 in a way similar as for all other engines. T_{vac}/W is calculated approximately 30% below the gas generator cycle, however, different assumptions in chamber pressure and nozzle expansion ratio. The explanation is mainly found in the more powerful and heavier turbopumps and the two

Table 27 Geometry data of LOX-LC3H8 staged combustion cycle engines from lrp1.1 calculation

Nozzle expansion ratio	–	23	33	120	180
Total engine length	m	2.9	3.25	5.39	6.52
Nozzle exit diameter	m	1.49	1.77	3.37	4.12
Total engine mass	kg	2691	2675	3114	3435
T_{vac}/W	-	83	83.5	76	69.9

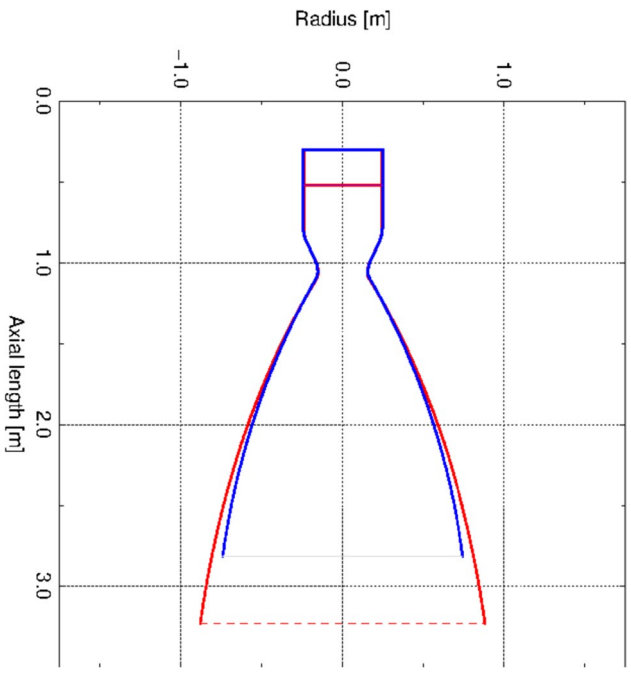

Fig. 12 Internal thrustchamber contours of LOX-LC3H8 staged combustion cycle engine $\varepsilon = 23$ (blue) and 33 (red)

high-pressure preburners. T_{vac}/W of the variant with expansion 33 is slightly above the engine with expansion 23 because of the latter's slightly larger massflow and hence size of major components.

The first stage engine-thrustchambers' internal flow contours as calculated by the DLR tool ncc under the assumption of parabolic nozzles with 80% fractional length are plotted as example of the staged combustion cycles in Fig. 12.

4 Engine data summary and evaluation

4.1 Impact of propellant combinations and cycle

The key performance drivers of chemical rocket engines are the choice of propellant combinations, the engine cycle and the nozzle expansion ratio. This section summarizes and compares data for the four selected fuels in combination with liquid oxygen and present these in a wide range of nozzle supersonic area ratios (15–180). Maximum achievable performances as well as characteristic differences are identified for the reference chamber pressure, mixture ratio and realistic design conditions previously described in Sects. 3.2–3.6.

The general trends of specific impulse of the open gas generator cycle engines with chamber pressure of 12 MPa are shown in Fig. 13 under vacuum and sea-level conditions. The largest nozzle expansion of 180 could provide up to 446 s I_{sp} in vacuum for LOX-LH2 while hydrocarbon propellants are not exceeding 350 s. Sea-level operation at expansion beyond ratios of 45 risk flow separation inside the nozzle and thus cannot be operated in first stage applications, even at full throttle. Reduced thrust levels with lower chamber pressures, as potentially required for controlled vertical landing of stages, are further restricting the feasible nozzle expansion. In case of the smallest nozzle, the I_{sp} at sea-level might reach up to 370 s for LOX-LH2 and hydrocarbon propellants are approaching a maximum of 290 s when selecting Methane as fuel.

The curves of the propellant combinations shown in Fig. 13 are running almost with constant distances in the displayed nozzle expansion range. The differences in vacuum I_{sp} between LH2 and LCH4 is roughly 90 s (deviation -3.6 s, + 6.2 s), between LCH4 and LC3H8 roughly 5 s (-1 s, + 0.5 s) and between LCH4 and RP1 about 10 s (-2 s, + 0.8 s). It is to be noted that such comparison is influenced by the assumption on the area ratio at which the chemical reactions are set to "frozen". Although reality is more complicated, the empirically based ratios depending on propellant are held constant for all nozzle sizes which

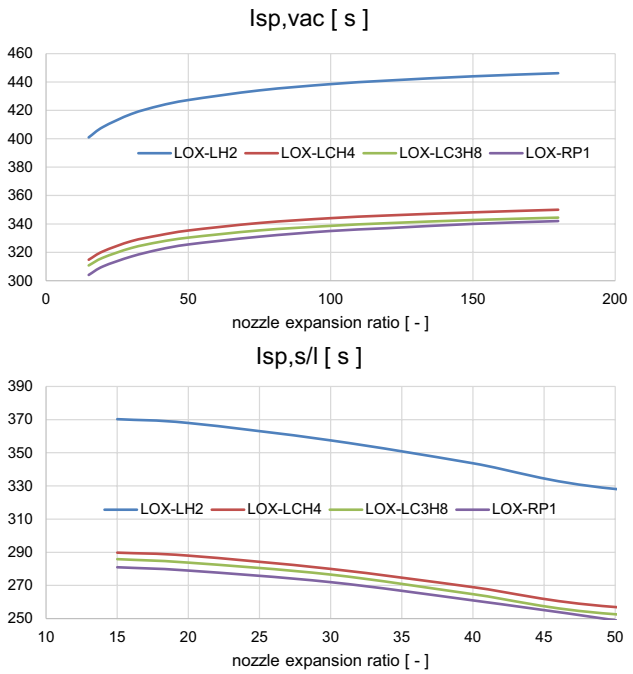

Fig. 13 Calculated specific impulse of open gas-generator cycle rocket engines as function of nozzle expansion ratio

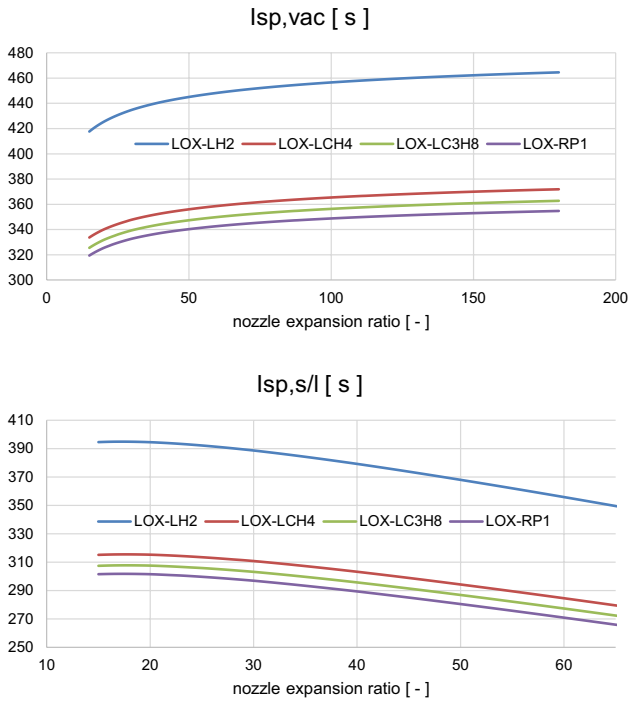

Fig. 14 Calculated specific impulse of staged-combustion cycle rocket engines as function of nozzle expansion ratio

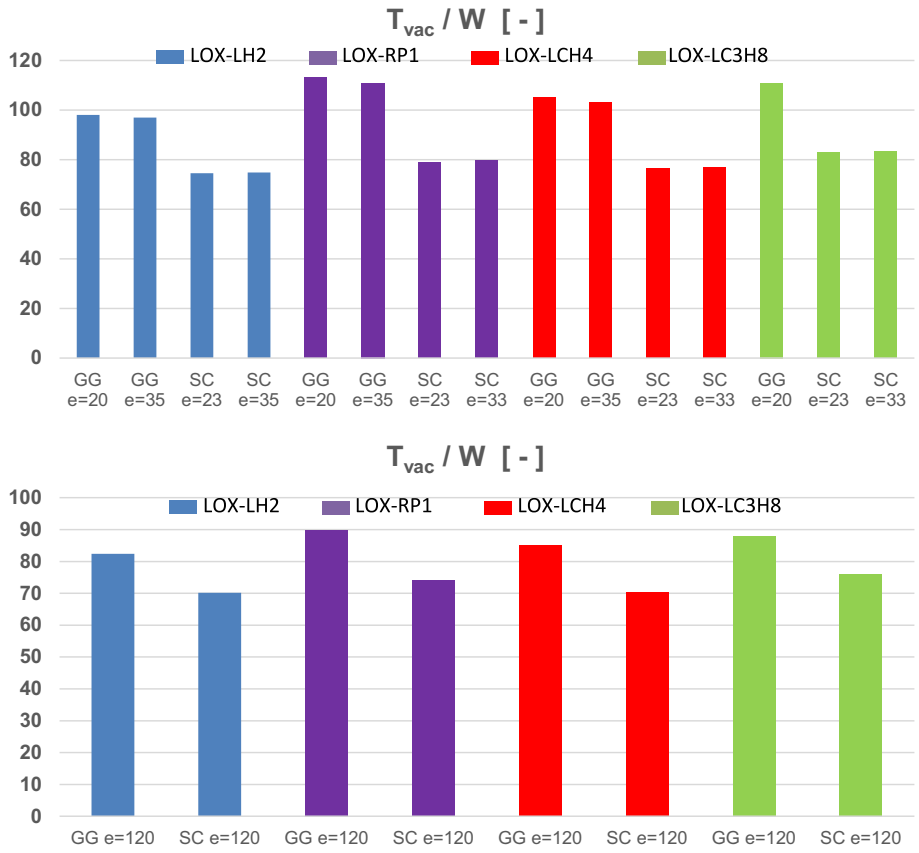

Fig. 15 Calculated thrust-to-weight ratios of selected reference engines for first stage (top) and upper stage application (bottom)

Table 28 Key performance data summary of selected first stage engines

	LOX-LH2 GG $\varepsilon = 20$	LOX-LH2 GG $\varepsilon = 35$	LOX-LH2 SC $\varepsilon = 23$	LOX-LH2 SC $\varepsilon = 35$	LOX-RP1 GG $\varepsilon = 20$	LOX-RP1 GG $\varepsilon = 35$	LOX-RP1 SC $\varepsilon = 23$	LOX-R1 SC $\varepsilon = 33$
Engine MR [−]	6	6	6	6	2.25	2.25	2.6	2.6
Sea level I_{sp} [s]	366	351	394	385	279	267	301	294
Vacuum I_{sp} [s]	405.5	418	428	437.8	310	320	327	334
Engine T_{vac}/W [−]	98.1	97	74.6	74.9	113	111	79	79.8

	LOX-LCH4 GG $\varepsilon = 20$	LOX-LCH4 GG $\varepsilon = 35$	LOX-LCH4 SC $\varepsilon = 23$	LOX-LCH4 SC $\varepsilon = 33$	LOX-LC3H8 GG $\varepsilon = 20$	LOX-LC3H8 SC $\varepsilon = 23$	LOX-LC3H8 SC $\varepsilon = 33$
Engine MR [−]	2.5	2.5	3.25	3.25	2.45	2.95	2.95
Sea level I_{sp} [s]	289	276	314	308	284	308	303
Vacuum I_{sp} [s]	320	331	342.5	349	315	335	342
Engine T_{vac}/W [−]	105	103	76.5	77	111	83	83.5

Table 29 Key performance data summary of selected upper stage engines

	LOX-LH2 GG $\varepsilon = 120$	LOX-LH2 SC $\varepsilon = 120$	LOX-RP1 GG $\varepsilon = 120$	LOX-RP1 SC $\varepsilon = 120$	LOX-LCH4 GG $\varepsilon = 120$	LOX-LCH4 SC $\varepsilon = 120$	LOX-LC3H8 GG $\varepsilon = 120$	LOX-LC3H8 SC $\varepsilon = 120$
Engine MR [−]	6	6	2.25	2.6	2.5	3.25	2.45	2.95
Vacuum I_{sp} [s]	440.4	458.6	338	353	348	366	344	362
Engine T_{vac}/W [−]	82.4	70.2	89.9	74	85	70.5	88	76

is sufficient for supporting the preliminary launcher sizing approach.

Similar trends derived for the staged combustion cycle with p_C of 16 MPa and the four propellant combinations are shown in Fig. 14. The largest nozzle expansion of 180 could provide up to 464 s I_{sp} in vacuum for LOX-LH2 while hydrocarbon propellants might reach 372 s at best with LOX-LCH4 achieving a slight edge over propane and kerosene. At the low end with nozzle ratio 15 the engines are slightly underexpanding even at sea-level. If not required by geometrical constraints, no rationale is found to choose a nozzle with area ratio below 18 in case of the staged combustion cycle with 16 MPa chamber pressure.

Similar to the gas generator cycle, the curves of the propellant combinations shown in Fig. 14 are running almost with constant distances in the displayed nozzle expansion range. The differences in vacuum I_{sp} between LH2 and LCH4 is roughly 90 s (deviation −6 s, +2.6 s), between LCH4 and LC3H8 roughly 8.5 s (with small deviations < 1 s) and between LCH4 and RP1 about 12 s (−1.4 s, +1.7 s). Note, the overall tendencies are robust while small deviations are subject to simplified assumptions on the chemical reactions in supersonic flow which should be treated with caution.

The impact of the cycle on performance has been checked assuming the typical chamber pressures of 12 MPa for the gas generator and 16 MPa for the staged combustion engines. The closed cycle brings a gain of 18–22 s in vacuum I_{sp}. The advantage of an increased chamber pressure pays off even more in case of sea-level operations with a specific impulse gain for the staged combustion cycle between 20 s ($\varepsilon = 15$) and 40 s ($\varepsilon = 45$).

4.2 Engine performance reference data for system analyses

The intended reusable launcher system analyses [2, 3] require the preselection of the most promising engines out of those preliminarily defined in Sects 3.3–3.6. In general, first stage engines projected to be used for vertical landing in VTVL-RLV have a smaller nozzle expansion than those to implemented in VTHL. This choice allows deep-throttling of engines without risking flow-separation in the nozzle to safely perform a vertical landing at roughly stage-T/W around 1.0. Engines to be used in horizontal landing RLV (VTHL) do not face such restrictions and somehow larger nozzle area ratios can be selected driven by optimal launcher ascent flight performance.

Preliminary mass estimation of all engines has been performed on main subcomponent level using empirically derived relationships implemented in DLR's *lrp* program. The launcher designs of [2, 3] scale the engine massflows individually per vehicle that a suitable number of first stage engines and a single upper stage engine of equivalent flow are defined. Vacuum thrust divided by engine weight is suitable for comparison of the different propellant and cycle options showing clear tendencies. The estimations deliver ambitious weight results compared to actual European heritage to date and the future will tell if such values are supported by actual engine design. On the other hand, announcements by SpaceX or weight targets of PROMETHEUS [37]. are even exceeding the calculated values of this study.

The high thrust to weight ratios estimated for all gas generator cycle engines should be noted, reaching from 97 (LOX-LH2) to 113 (LOX-RP) for first stages (Fig. 15). The staged combustion cycle engines are between 25 and 30% below the open cycle due to the significantly raised pressure levels and turbopump power. A ranking comparison of T_{vac}/W between the propellants is slightly correlated with the bulk density. In this mass estimation the difference is less than 15% for similar engine types because the more complex LOX-LH2-engines with increased specific power required by the hydrogen pump and hence mass growth is widely compensated by the reduced massflow needed by this propellant combination for the same thrust level.

In case of the upper stage engines with large expansion nozzle, the differences between the propellants are even less pronounced with maximum difference less than 10%.

All key performance reference data of the first stage engines selected for the RLV system analyses are listed in Table 28. In a similar way the reference data of the upper stage engines are listed in Table 29.

5 Conclusion

Several variations of advanced liquid-propellant rocket engines have been performed to support an RLV-system study with reliable and realistic propulsion data. The three cryogenic propellants hydrogen, methane and propane as well as kerosene (RP1) have been used in combination with LOX as oxidizer. Open gas-generator cycle and closed staged combustion cycle types were defined with relevant chamber pressures and nozzle expansion ratios.

Expendable upper stage engines have been derived from the reusable first stage engines keeping all internal cycle parameters, however, with significantly increased nozzle size for improved performance. With the intention of maximizing I_{sp}, initially, nozzle expansion ratios have been extended up to 180. The extremely large nozzles of the high-thrust engines turn out to be challenging from manufacturing-, weight- and integration perspective. In order to keep realistic assumptions, the expansion ratios have been restricted to 120 loosing roughly 5 s of vacuum I_{sp}.

A systematic comparison of the different engines in a large range of nozzle expansion shows the combination LOX-LH2 about 90 s ahead of LOX-LCH4 closely followed by LOX-LC3H8 and LOX-RP1 with the latter having a distance of roughly 10 s to methane. A closed-cycle staged combustion engine brings around 20 s I_{sp} gain in vacuum and up to 40 s in sea-level operations. However, the less performing hydrocarbon- and open-cycle gas-generator engines offer a better thrust-to-weight-ratio than hydrogen and staged combustion. The question which of the characteristics become dominating in future launchers needs to be addressed in multi-disciplinary investigations under consideration of relevant missions.

Therefore, the optimum engine for a future European partially reusable space transportation system cannot be selected solitarily out of engine characteristics. The preselected promising engine candidates of this paper are transferred to a system study on different types of partially reusable space transportation vehicles. This multidisciplinary study with sufficiently detailed analyses also on subsystem level should provide a reliable technical basis for the development decisions on the next generation of advanced launch vehicles.

Author contributions MS: performed all calculations, data post processing and analyses, has written almost the complete manuscript, reviewed the complete manuscript several times. reworked the complete manuscript. JW: reviewed the complete manuscript, contributed to the manuscript by research on state-of-the-art in similar propulsion analyses and contributed section on near triple point propellant characteristics and interest. checked the reworked manuscript.

Funding Open Access funding enabled and organized by Projekt DEAL.

Data availability No datasets were generated or analysed during the current study.

Declarations

Conflict of Interest The authors declare no competing interests.

Open Access This article is licensed under a Creative Commons Attribution 4.0 International License, which permits use, sharing, adaptation, distribution and reproduction in any medium or format, as long as you give appropriate credit to the original author(s) and the source, provide a link to the Creative Commons licence, and indicate if changes were made. The images or other third party material in this article are included in the article's Creative Commons licence, unless indicated otherwise in a credit line to the material. If material is not included in the article's Creative Commons licence and your intended use is not permitted by statutory regulation or exceeds the permitted use, you will need to obtain permission directly from the copyright holder. To view a copy of this licence, visit http://creativecommons.org/licenses/by/4.0/.

References

1. Dietlein, I., Bussler, L., Stappert, S., Wilken, J., Sippel, M.: Overview of system study on recovery methods for reusable first stages of future European launchers. CEAS Space J. (2024). https://doi.org/10.1007/s12567-024-00557-9
2. Wilken, J., Stappert, S.: Comparative analysis of european vertical-landing reusable first stage concepts. CEAS Space J. (2024). https://doi.org/10.1007/s12567-024-00549-9
3. Bussler, L., Sippel, M., Dietlein, I., Wilken, J., Stappert, S.: Comparative analyses of European horizontal-landing reusable first stage concepts. Submitted to CEAS Space Journal (2024)
4. Stappert, S., Dietlein, I., Wilken, J., Bussler, L., Sippel, M.: Options for future european reusable booster stages: evaluation and comparison of VTHL and VTVL return methods. Submitted to CEAS Space Journal (2024)
5. Sutton, G.P., Biblarz, O.: Rocket Propulsion Elements. John Wiley & Sons, Hoboken (2016)
6. Castellini, F.: Multidisciplinary Design Optimization for Expendable Launch Vehicles, Ph.D. Thesis. Polytechnic University of Milan, Milan (2012)
7. Burkhardt, H., Sippel, M., Herbertz, A., Klevanski, J.: Comparative Study of Kerosene and Methane Propellant Engines for Reusable Liquid Booster Stages, 4th International Conference on Launcher Technology Space Launcher Liquid Propulsion, Liege (Belgium) (2002)
8. Burkhardt, H., Sippel, M., Herbertz, A., Klevanski, J.: Kerosene vs methane: a propellant tradeoff for reusable liquid booster stages. J. Spacecr. Rockets (2004). https://doi.org/10.2514/1.2672
9. Preclik, D., Hagemann, G., Knab, O., Brummer, L., Mäding, C., Wiedmann, D., Vuillermoz, P.: LOX/Hydrocarbon Propellant Trade Considerations for Future Reusable Liquid Booster Engines, AIAA 2005–3567, 41st AIAA/ASME/SAE/ASEE Joint Propulsion Conference & Exhibit, Tucson, Arizona (2005)
10. Burkhardt, H., Herbertz, A., Sippel, M., Woschnak, A., Riccius, J.: Evaluation of green propellants for space applications, WP 2200: propulsion requirements, DLR-IB 647–2, SART TN-003/2004 (2004), Available at https://elib.dlr.de/1716/1/SART-TN3-2004.pdf
11. Li, X., Ma, X., Zhang, J., et al.: Review of hydrogen embrittlement in metals: hydrogen diffusion, hydrogen characterization, hydrogen embrittlement mechanism and prevention. Acta Metall. Sin. **33**, 759–773 (2020). https://doi.org/10.1007/s40195-020-01039-7
12. NN: NIST Chemistry WebBook, SRD 69, https://webbook.nist.gov/chemistry/fluid/. https://doi.org/10.18434/T4D303
13. Maeda, T., Onga, T., Tamura, T., Negoro, N., Okita, K., Kobayashi, T., Kawashima, H.: Firing Tests of LE-9 Development Engine for H3 launch vehicle, IAC-19-C4.1.4, 70th International Astronautical Congress (IAC), Washington D.C., United States, 21–25 October 2019
14. Sippel, M., Herbertz, A., Haeseler, D., Götz, A.: Feasibility of High Thrust Bleed Cycle Engines for Reusable Booster Applications; 4th International Conference on Launcher Technology & Space Launcher Liquid Propulsion, Liege (2002)
15. Sippel, M., Herbertz, A., Manfletti, Ch., Burkhardt, H., Imoto, T., Haeseler, D., Götz, A.: Studies on Expander Bleed Cycle Engines for Launchers, AIAA 2003–4597, 39th AIAA/ASME/SAE/ASEE Joint Propulsion Conference and Exhibit, Huntsville, Alabama (2003)
16. Zeleznik, F.J., Gordon, S.: A general IBM 704 or 7090 computer program for computation of chemical equilibrium compositions, rocket performance, and Chapman-Jouguet detonations. NASA TN D-1454 (1962)

17. Gordon, S., McBride, B.J.: Computer program for calculation of complex chemical equilibrium compositions, rocket performance, incident and reflected shocks, and Chapman-Jouguet detonations, NASA SP-273, 1971, Interim Revision (1976)
18. Gordon, S., McBride, B.J.: Computer program for calculation of complex chemical equilibrium compositions and applications I. Analysis. NASA-RP-1311 (1994)
19. Gordon, S., McBride, B.J.: Computer program for calculation of complex chemical equilibrium compositions and applications II. User's manual and program description. NASA RP-1311-P2 (1996)
20. Ponomarenko, A.: RPA - Tool for rocket propulsion analysis, C++ Implementation (2010)
21. Ponomarenko, A.: RPA: tool for rocket propulsion analysis, assessment of delivered performance of thrust chamber, (v.1). https://www.rocket-propulsion.com/downloads/pub/RPA_AssessmentOfDeliveredPerformance.pdf (2013). Accessed March 2013
22. Gamgami, F., Sippel, M., Dumont, E.: Statistical analysis and classification of rocket motor efficiency, thrust to mass ratio and structural index, internal report SART TN-007/2009
23. Ponomarenko, A.: RPA - Tool for Rocket Propulsion Analysis, Space Propulsion 2014. Cologne, Germany (2014)
24. Ponomarenko, A.: RPA: Tool for Rocket Propulsion Analysis, Thermal Analysis of Thrust Chambers. https://www.rocket-propulsion.com/downloads/pub/RPA_ThermalAnalysis.pdf (2012). Accessed July 2012
25. Nickerson, G. R., Dang, L. D., Coats, D. E.: Engineering and programming manual: two-dimensional kinetic reference computer program (TDK), NASA-CR-178628 (1985)
26. RS-68, https://en.wikipedia.org/w/index.php?title=RS-68&oldid=838191803 (2018). Accessed May 20, 2018
27. Sippel, M., Yamashiro, R., Cremaschi, F.: Staged combustion cycle rocket engine design trade-offs for future advanced passenger transport, ST28–5, Space Propulsion 2012, Bordeaux (2012)
28. Yamashiro, R., Sippel, M.: Preliminary design study of staged combustion cycle rocket engine for spaceliner high-speed passenger transportation concept, IAC-12-C4.1.11, Naples (2012)
29. Sippel, M., Schwanekamp, T., Ortelt, M.: Staged Combustion Cycle Rocket Engine Subsystem Definition for Future Advanced Passenger Transport, Space Propulsion 2014. Cologne, Germany (2014)
30. Sippel, M., Wilken J.: Preliminary Component Definition of Reusable Staged-Combustion Rocket Engine, Space Propulsion 2018 conference, Seville (2018)
31. Sippel, M., Stappert, S., Pastrikakis, V., Barannik, V., Maksiuta, D., Moroz, L.: Systematic Studies on Reusable Staged-Combustion Rocket Engine SLME for European Applications, Space Propulsion 2022. Estoril, Portugal (2022)
32. Jeaugey, I., Montheillet, J., Reichstadt, S., Ghouali, A., Dantu, G.: System engineering presentation of the european staged combustion demonstrator score-D, Space Propulsion 2012, Bordeaux (2012)
33. NN: Space shuttle main engine orientation, Boeing Rocketdyne propulsion & power, space transportation system training data (1998)
34. Deeken, J., Herbertz, A.: Vergleich von Expanderzyklusvarianten und Turbomaschinenanordnungen in Raketentriebwerken unter Verwendung des Zyklusanalyseprogramms LRP, DLR–IB 647–2004 /07, SART TN-013/2004, internal report in German (2004)
35. RD-120, https://en.wikipedia.org/wiki/RD-120 (2020). Accessed May 22, 2020
36. LandSpace: creator of commercial space transportation systems, fact sheet, undated (2023)
37. P. Simontacchi: Prometheus: precursor of new low-cost rocket Engine Family, Space Propulsion 2018 conference, Seville (2018)
38. Wilken, J.; et al: Critical Analysis of SpaceX's Next Generation Space Transportation System: Starship and Super Heavy, 2nd HiSST: International Conference on High-Speed Vehicle Science Technology, Bruges (2022)
39. Wilken, J., Scelzo, M., Peveroni, L.: System Study of Slush Propellants for Future European Launch Vehicles, Space Propulsion 2018 conference, Seville (2018)

Publisher's Note Springer Nature remains neutral with regard to jurisdictional claims in published maps and institutional affiliations.